Regulating Metabolic Energy Among Joints During Human Walking Using a Multiarticular Unpowered Exoskeleton

Tiancheng Zhou, Caihua Xiong, *Member, IEEE*, Juanjuan Zhang, *Member, IEEE*, Wenbin Chen, *Member, IEEE*, and Xiaolin Huang

***Abstract*— Researchers have found that the walking economy can be enhanced by recycling ankle metabolic energy using an unpowered ankle exoskeleton. However, how to regulate multiarticular energy to enhance the overall energy efficiency of humans during walking remains a challenging problem, as multiarticular passive assistance is more likely to interfere with the human body's natural biomechanics. Here we show that the metabolic energy of the hip and knee musculature can be regulated to a more energy-effective direction using a multiarticular unpowered exoskeleton that recycles negative mechanical energy of the knee joint in the late swing phase and transfers the stored energy to assist the hip extensors in performing positive mechanical work in the stance phase. The biarticular spring-clutch mechanism of the exoskeleton performs a complementary energy recycling and energy transfer function for hip and knee musculature. Through the phased regulation of the hip and knee metabolic energy, the target muscle activities decreased during the whole assistive period of the exoskeleton, which was the direct reason for 8.6 ± 1.5% (mean ± s.e.m) reduction in metabolic rate compared with that of walking without the exoskeleton. The proposed unpowered exoskeleton enhanced the user's multiarticular energy efficiency, which equals improving musculoskeletal structure by adding a complementary loop for efficient energy recycling and energy transfer.**

***Index Terms*— Multiarticular unpowered exoskeleton, metabolic energy, energy transfer, human walking, human response.**

Manuscript received July 21, 2020; revised December 1, 2020 and February 10, 2021; accepted March 8, 2021. Date of publication March 10, 2021; date of current version March 22, 2021. This work was supported in part by the National Natural Science Foundation of China under Grant 52027806, Grant U1913601, Grant 91648203, and Grant U1913205. *(Corresponding author: Caihua Xiong.)*

Tiancheng Zhou, Caihua Xiong, and Wenbin Chen are with the State Key Laboratory of Digital Manufacturing Equipment and Technology, Institute of Rehabilitation and Medical Robotics, Huazhong University of Science and Technology, Wuhan 430074, China (e-mail: chxiong@hust.edu.cn).

Juanjuan Zhang is with the Institute of Robotics and Automation Information System, Nankai University, Tianjin 300071, China, and also with the Tianjin Key Laboratory of Intelligent Robotics, Nankai University, Tianjin 300071, China.

Xiaolin Huang is with Department of Rehabilitation Medicine, Tongji Hospital, Tongji Medical College, Huazhong University of Science and Technology, Wuhan 430074, China.

This article has supplementary downloadable material available at https://doi.org/10.1109/TNSRE.2021.3065389, provided by the authors.

Digital Object Identifier 10.1109/TNSRE.2021.3065389

I. Introduction

WALKING is the most common means of locomotion in human daily life. With evolution occurring over generations and humans having taken thousands of steps a day, the human musculoskeletal system is considered to be well adapted to walking [1]. However, the apparent efficiencies of the ankle, knee and hip musculature in converting metabolic energy to positive mechanical work during walking are still not perfect, only 61%, 24% and 24% respectively [2]. Low efficiency is also one of the major factors limiting locomotion performance. Although it is difficult to alter the human musculoskeletal structure, people are searching for other ways to regulate human metabolic energy to a more energy-efficient manner using wearable exoskeletons.

In the past six years, researchers have made advancements in enhancing the walking economy by regulating metabolic energy using unpowered and powered exoskeletons [3]. Moreover, researchers have found that biological joint power can be partly replaced by external power input using autonomous powered exoskeletons [4]–[7], thus reducing the overall metabolic energy of walking. In addition, the parameters sweeping [8]–[10] and human-in-the-loop optimization studies [11], [12] on tethered powered exoskeletons have also demonstrated the potential to further reduce the metabolic cost of walking by optimizing assistive parameters. Although the powered exoskeletons can provide humans with substantial mechanical energy in replace of the biological mechanical work, there is a trade-off between assistance duration and metabolic penalty caused by the mass of the batteries and motor combinations [9], [13], [14].

As alternatives, unpowered exoskeletons, which can get rid of the external energy source and metabolic penalties of exoskeleton mass, seek another way of improving human-exoskeleton efficiency overall [13], [15]–[17]. Researchers have found that the walking economy can be enhanced by reducing the muscle effort needed to generate force using an unpowered ankle exoskeleton [15]. However, how to regulate multiarticular metabolic energy remains a challenging problem. First, the assistance effect is more likely to be offset by the metabolic penalty of exoskeleton mass. The structures of multiarticular unpowered exoskeletons are

more complex than those of single joint exoskeletons, which means that the exoskeleton mass and inertia are higher for the lower limb [16]. The mass and inertia added on the lower limb, especially on the distal joint, will affect joint kinetics and cause metabolic penalty [18], which are more likely to offset the assistance effect. A quasi-passive exoskeleton has been proposed to augment human load carrying capacity by transferring the load to the ground while providing assistive torque for each joint, but the experiment also showed a 10% metabolic increase due to the metabolic penalty of extra inertia and mass added on lower limb [16]. Moreover, the multiarticular assistance is more likely to interfere with the natural biomechanics and natural energy transfer of the lower limb during human walking. Humans not only exploit biological tendons to recycle energy for enhancing the energy efficiency of a single joint but also transfer energy between joints through lower limb segments and bi-articular muscles to enhance the overall energy efficiency of multiple joints [19]. However, researchers mainly focused on the energy recycling function of multiarticular unpowered exoskeletons in earlier studies [13], [16], neglecting natural energy transfer in lower limb musculature. In a previous study, an multiarticular exoskeleton assisted the hip and ankle joints to recycle energy in a coupled manner [13]. Although the exoskeleton reduced biological joint torques, the metabolic cost increased, possibly due to the interference in the natural energy storage and energy transfer of the human tendons and bi-articular muscles [13]. In fact, recent studies have demonstrated the potential of facilitating energy transfer using bi-articular tethered powered knee-ankle exoskeleton [20] and quasi-passive knee-ankle exoskeleton [21]. The results showed that the biological effort of ankle muscles could be further reduced with the additional energy collected from the knee joint by the exoskeleton. Therefore, when developing multiarticular unpowered exoskeletons, we should not only simplify the exoskeleton structure to minimize the metabolic penalty caused by the exoskeleton mass and inertia but also attach importance to the energy transfer function of the exoskeleton.

Regarding the musculature of the human lower limb, in addition to biological tendons, bi-articular muscles are also essential contributors to walking economy, and play an important role in recycling and transferring energy during human locomotion [19]. Bi-articular muscles can not only act like biological tendons to recycle energy but also transfer energy produced by mono-articular muscle from proximal joint to distal joint [22], [23]. For example, during leg extension, mechanical energy produced by the gluteus maximus (mono-articular hip extensor) is transferred through hamstrings (bi-articular muscles) to the knee joint [24], [25]. Besides, the transfer of energy from the proximal joint to the distal joint makes the muscle volume distribution more concentrated at proximal joint, thus reducing the energy consumption of moving leg [24]. Furthermore, the double joint actuation of bi-articular muscles allows negative joint power, partly dissipated due to friction of muscle bundles, to be utilized at the adjacent joint that requires positive power [26], [27]. In conclusion, bi-articular muscles are essential contributors to walking economy due to their functions of tendon-action, energy transfer and double joint actuation. These functional characteristics make it possible to recycle and transfer energy among multiple joints in different gait phases, thus enhancing multiarticular energy efficiency. In turn, exoskeletons with complementary double actuation and energy transfer capabilities may also be effective in regulating multiarticular metabolic energy.

To regulate multiarticular energy and enhance the overall walking economy, we first analyzed the energy characteristics and power curves of lower limb joints. Then, we developed a hip-knee unpowered exoskeleton that can transfer energy between the hip and knee in a complementary manner (Fig. 1). The bi-articular spring-clutch of the exoskeleton assists the user to recycle negative mechanical energy from the knee joint in the late swing phase. In the stance phase of the next gait cycle, the stored energy was released to assist the gluteus maximus (mono-articular hip extensor) in performing positive mechanical work, ultimately regulating multiarticular energy across different gait phases. To evaluate the human response to the proposed multiarticular assistance principle, we measured and statistically evaluated metabolic rate, muscle activity and joint mechanics under different spring stiffness conditions in nine healthy adults (Fig. 2). We also performed speed experiments to evaluate the generality of this assistance principle within a range of walking speeds.

II. Materials and Methods

A. Analysis of Human Walking Biomechanics

As mentioned above, the apparent efficiencies of hip and knee joints are nearly 24% [2], which are much lower than that of ankle joint. Learning from the anatomy and kinesiology of the lower limb, the ankle plantar flexors have short fibers and work with long elastic tendons. This muscle-tendon architecture shows a characteristic of high fixed-end compliance [28], storing and returning energy in an economical way. In contrast, hip extensors and knee muscles, which do not work with long elastic tendons, are more suitable for performing muscle fiber work but at low efficiency [29]. The peak energy efficiency of positive muscle work is merely 25%, which is much lower than the efficiencies of producing negative muscle work (nearly -120%) and generating isometric force [30]. This may suggest that there is much room for improvement in the energy efficiency of the knee and hip musculature. The simulation results showed that the muscle efficiency can be enhanced by 3% and metabolic cost can be reduced by 7.1% by assisting hip flexion with an elastic hip exoskeleton [31]. It was found that the metabolic cost of older adults can be reduced with the assistance of an elastic hip flexion device [32]. Haufe et al found that the biological hip power and muscle activity of soleus were reduced with the assistance of passive hip springs during walking [33]. So, in addition to ankle unpowered exoskeleton [15], the elastic exoskeleton may also be used to assist hip and knee musculature to improve the efficiency of the human–machine system as a whole.

During walking, hip and knee musculature shows a different energy consumption characteristic. The major function of knee muscle-tendons is energy absorption (i.e. negative work). The previous study on harvesting negative mechanical

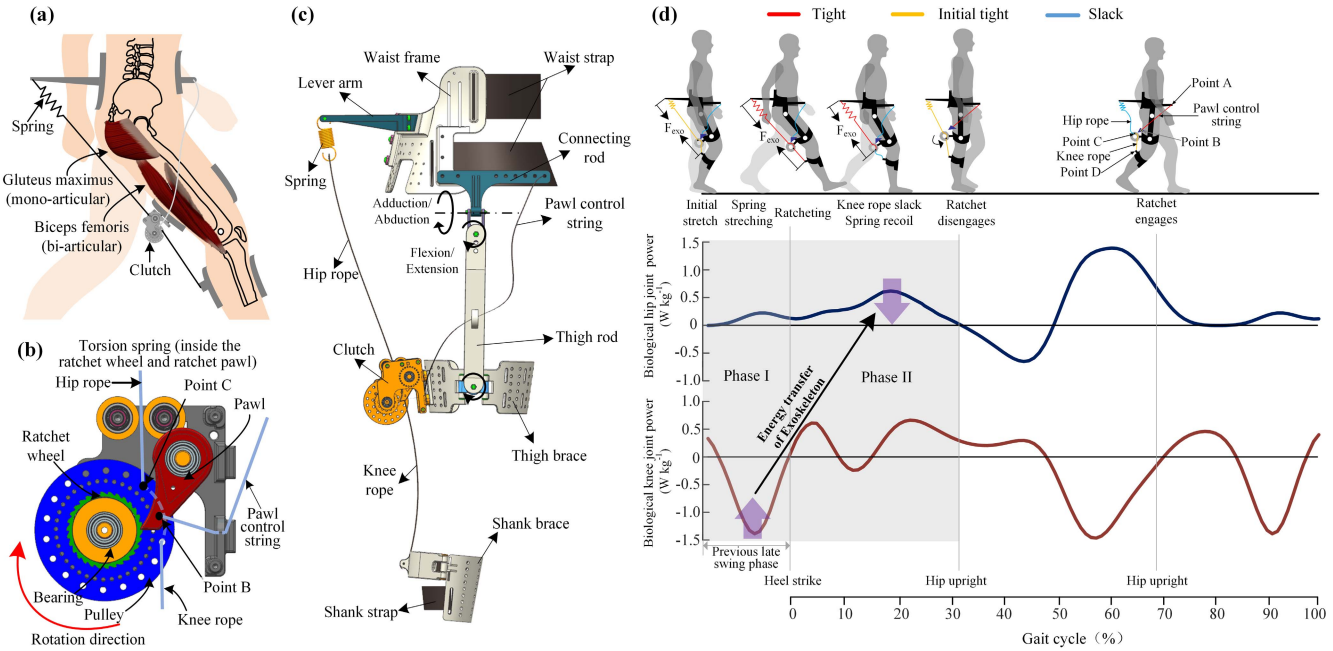

Fig. 1. **Multiarticular passive exoskeleton design.** (a) The bi-articular spring-clutch acts in parallel with target gluteus maximus and biceps femoris. (b) The mechanical clutch is composed of ratchet wheel and ratchet pawl that engage the spring when the hip joint is in flexion and disengage it when the hip joint is in extension. (c) Mechanical structure of the multiarticular exoskeleton. The exoskeleton is composed of rigid frames attached to human waist, thigh and shank. (d) The assistive principle of the exoskeleton. During phase I, the spring absorbs negative mechanical energy of knee joint with knee extension while providing hip joint with extension torque passively. During phase II, knee rope will be slack as the knee joint flexes and engagement of clutch prevent ratchet wheel from rotating in reverse direction. So, the energy stored in spring will be released to only assist hip joint with hip extension. When the hip joint extends to up-right position, the pawl control string begins to pull the ratchet pawl to disengage the clutch and allow free movement of hip and knee joint. The detailed working process of mechanical clutch is presented in Materials and Methods.

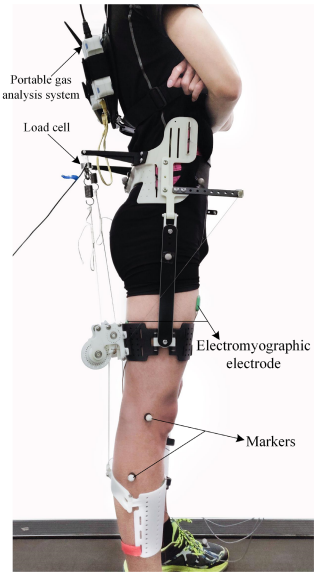

Fig. 2. Participant wearing the multiarticular exoskeleton. The exoskeleton is composed of rigid frames attached to human waist, thigh and shank. Muscle activities, lower limb motion and spring force were measured.

energy of knee joint to generate electricity found that it would cost less energy penalty compared to harvesting positive mechanical energy [34], which also means that exoskeleton may recycle energy from negative mechanical energy of knee joint with minimal penalty. In contrast, the major function of hip muscle-tendons is energy production (i.e. positive work). The amount of positive work produced by hip muscle-tendons is nearly equal to that of ankle joint but with a low efficiency. Therefore, we can exploit the exoskeleton to assist knee musculature to absorb energy and then transfer the stored energy to assist hip musculature to do positive mechanical work, thus reducing metabolic energy for positive mechanical work. Specifically, the knee joint negative power reaches its peak in the late swing phase (Fig. 1d). During this phase, the hamstrings and gastrocnemius (bi-articular muscles) mainly do negative mechanical work on the knee joint to slow down knee extension for coming heel strike. In the following stance phase of the same leg, positive mechanical power of the hip joint reaches its peak (Fig. 1d), which is also the major energy consumption period of hip extensors [35]. The gluteus maximus (mono-articular hip extensor) and hamstrings (bi-articular muscle) mainly provide hip joint with extension torque and do positive mechanical work to pull the leg.

B. Assistive Principle of Hip-Knee Unpowered Exoskeleton

According to the analysis above, we proposed a hip-knee unpowered exoskeleton (Fig. 1c) that exploits the bi-articular clutch-spring mechanism to regulate metabolic energy of hip and knee in different gait phases. As shown in Fig. 1d, the knee extension stretches spring during the late swing phase while the hip angle nearly remains constant. During this phase (phase I), the exoskeleton spring passively stores

TABLE I
UNPOWERED HIP-KNEE EXOSKELETON MASS DISTRIBUTION

Segment	Mass (g)
Waist frame (including level arm)	690
Thigh segments(x2)	300
Shank segments(x2)	220
Average spring mass	70
Mechanical clutch(x2)	580
Total mass (biarticular sum)	**1860**

part of negative mechanical energy of knee joint while providing the hip with extension torque. Between phase I and II, the mechanical clutch changes the target assistance joint from hip and knee joints to hip joint, thus equivalently completing the function of energy transfer. In the next stance phase (phase II), the spring releases the stored energy to only assist hip extensors in performing positive mechanical work on hip joint. The clutch is an important controller to fulfill the phased regulation function of proposed exoskeleton. If the exoskeleton spring works without the clutch, the exoskeleton will only couple to assist hip extension and knee flexion during the whole assistive period. The exoskeleton will provide the knee joint with flexion torque during the energy releasing phase, which may interfere with the natural biological knee extension torque. In all, the exoskeleton provides humans with a complementary loop that passively recycles negative mechanical energy of knee joint to assist hip extensor in doing positive mechanical work. Through energy recycling and energy transfer, the exoskeleton aims to regulate the metabolic energy of hip and knee musculature to an energy-effective direction.

C. Design of Hip-Knee Unpowered Exoskeleton

As shown in Fig. 1c, the exoskeleton has three main parts: waist frame, thigh segments and shank segments. The waist frame connects to the thigh segment by two hinge joints in serial, which enable flexion/extension and adduction/abduction of hip joint. As the flexion and extension of knee joint are not simple rotation movement [36], the thigh segment and shank segment of our exoskeleton are set apart to prevent the undesired forces due to misalignment between biological knee joint and exoskeleton joint, which was emphasized by Mooney *et al.* [4]. For our exoskeleton, the lever arm of the hip joint was set as 30 cm, which is five times of lever arm at the knee joint. During phase I, the exoskeleton spring spans across the hip and knee, simultaneously providing assistive torque on both joints. On the one hand, the lever arm of the hip joint changes the direction of the spring force direction to increase the exoskeleton torque on the hip joint. On the other hand, the short lever arm of knee joint reduces the exoskeleton torque that hinders knee extension during leg swing. The detailed mass distribution is present in Table I. Most exoskeleton mass is concentrated near the waist, minimizing the metabolic penalty of external mass. The detailed exoskeleton mechanism is presented in the Supplementary Material.

D. Detailed Working Process of Mechanical Clutch

The mechanical design of the clutch was inspired by [15]. As shown in Fig. 1b, the mechanical clutch is composed of the ratchet wheel and ratchet pawl. When the clutch is engaged, the ratchet wheel can only rotate in a clockwise direction. The engagement of the clutch is controlled by the hip joint angle during walking. Specifically, the proximal end of the pawl control string is connected to the rod (Point A, Fig. 1d) on the waist frame and the distal end of the pawl control string is connected to the ratchet pawl at point B (Fig. 1b). The initial tight position of the pawl control string is the hip up-right position. When the hip joint is in extension position, the distance between A and B is longer than the length of pawl control string and ratchet pawl will be pulled to be disengaged. When the hip joint is in flexion position, the clutch is always engaged. The proximal end of the spring is connected to lever arm on the waist, and the distal end of spring is connected to ratchet wheel at point C through a hip rope. The proximal end of the knee rope is connected to ratchet wheel at point C and distal end of knee rope is connected to shank frame at Point D. As shown in Fig. 1d, the initial tight position (initial tight) of the knee rope and hip rope is at maximum flexion position of knee joint during the leg swing. During the energy storage phase (phase I), the hip angle nearly remains constant and the knee extension stretches spring. The spring stores part of the knee mechanical energy and assists knee flexors to slow down knee extension for coming heel strike. Meanwhile, the spring passively applies extension torque for hip joint. At the end of phase I, the knee joint extends to its maximum angle, and the distance between C and D reaches its maximum length. After the heel strike, the knee joint naturally flexes to cushion the loads, and the distance between C and D decreases. As the clutch is engaged and the ratchet wheel cannot rotate in an anticlockwise direction, the knee rope is slack. Thus, the spring torque only applies to hip joint during energy releasing phase (Phase II). The stored energy is released to assist hip extensors in performing positive mechanical work with hip extension movement. When the hip joint extends to the upright position, the pawl control string begins to pull the ratchet pawl, and the clutch is disengaged. As the torsional spring is embedded in the ratchet wheel (Fig. 1b), point C returns to the initial position when the clutch disengages. The knee rope is still under small force applied by torsional spring. When the hip joint flexes to flexion position, the torsion spring in the pawl will reset the clutch to be engaged. For each participant, we will first measure the maximum knee flexion angle and hip angle at the same time before experiment. As shown in Fig.1d, we will adjust the initial length of hip rope and knee rope in this posture (beginning of Phase I). The pawl control string is only controlled by hip angle, so we adjust the initial length of pawl control string in the hip upright posture. The biarticular spring-clutch is based on the specific working process of our exoskeleton. For different assistive principles, different mechanical or electronic clutches based on the traditional ratchet mechanism, may be customized. The detailed design parameters of our clutch are presented in the Supplementary Material.

E. Experimental Protocol

Nine healthy male adults (N = 9, age 24.9 ± 3.7 years, weight 66.9 ± 8.7 kg, height 1.76 ± 0.05m) participated in the experiment. No statistical methods were used to predetermine sample size, and it was selected according to standard practice for locomotion research. The participants were recruited randomly with no need to consider the particular body size (e.g. height and weight), as the connection parts of the exoskeleton can be adjusted in size. Blinding was not practical in this protocol. The timing of the experiments, such as morning, afternoon, or evening, is a potential source of bias. All participants provided written consent before the experiments and completed the experiments only once. There was no missing data in the formal experiment. The study was approved by the ethics committee of the Tongji Medical College.

In the preliminary assessment of metabolic energy in the conference paper [37], we tested a series of spring stiffness and found the inflection point where the metabolic energy changes with the spring stiffness. To find the relationship between the spring stiffness and net metabolic rate, we added experimental conditions for springs with greater stiffness. We also synchronously measured the metabolic rate, EMG and kinematic data in the selected spring stiffness conditions.

The experimental protocol involved three sessions: walking habituation (session I), walking with different spring stiffness on the treadmill (session II), walking on the force plate at preferred speed (session III). Each session was performed on a separate day to avoid fatigue effects. The stiffness of springs was selected based on the preliminary experimental result [37] within the range of biological stiffness of hip and knee joints [38], [39]. The stiffnesses of the spring were 1.5, 3.0, 4.0, 4.8 kN m^{-1}. As the length of the lever arm was 0.3 m, the equivalent rotational stiffnesses for hip joint were 135, 270, 360, 432 N·m Rad^{-1}. In session I, participants adapted themselves to each stiffness twice, and each waking trial lasted 6 minutes on the treadmill at the speed of 1.5 m s^{-1}. Participants could rest 5 minutes between the habituation trials. In session II, participants walk with different spring stiffness to test the effect of assistance magnitude on metabolic rate. Before the formal test, participants stand still for basic metabolic rate measurement. After that, participants adapted themselves to spring stiffnesses and each stiffness for two minutes in random order. After a 5-minute break, the participants began formal experiments. The formal test involves six 6-minute conditions: 4 spring stiffness conditions, one walking with exoskeleton but no assistance condition (NA, k = 0 N·m Rad^{-1}) and one walking with no exoskeleton condition (NE). Participants rested 5 minutes between each condition. The walking conditions were in random order to minimize the learning effect. The last 2-minute data of each condition were analyzed. After all participants complete session II, they were recruited to walking with the optimal spring stiffness at preferred speed on the force plate (session III). This session aims to test whether the exoskeleton significantly changes the human natural walking gait, including preferred walking speed and joint mechanics. This session included two conditions: walking with optimal spring stiffness at the preferred speed, walking with no exoskeleton at preferred speed on the force plate. The subjects walked on the force plate at preferred speed for twenty gait cycles and we used 10 steady-state gait cycles for analysis.

As human walks at different speeds in daily life, we recruited the same 9 participants to perform speed experiments to demonstrate the generality of the proposed passive method for different walking speeds. Participants first performed a 6-minute standing trial for basic metabolic rate data and warm-up trials. In the walking testing session, the warm-up trials involved four 2-minute walking trials with the optimal spring stiffness for different walking speeds. After a 5-minute break, participants performed four 6-minute testing trials for metabolic data: 1 m s^{-1}, 1.25 m s^{-1}, 1.5 m s^{-1}, 1.75 m s^{-1} conditions, and another four matched group: walking with no exoskeleton at these four speeds. The participants took a 5-minute rest between each testing trial. The order of experimental conditions was randomized to minimize the effect of order. We analyzed the experimental data in the last 2 minutes of each trial.

F. Biomechanical and Metabolic Measurements

We used an indirect calorimetry system (Oxycon Mobile, CareFusion) to measure oxygen consumption and carbon dioxide production during walking. Lower limb motions were measured by a reflective marker motion capture system (Vicon, Oxford Metrics; 100Hz). Lower limb muscle activity (soleus, medial gastrocnemius, anterior tibialis, rectus femoris, biceps femoris muscle, gluteus maximus) was recorded by an electromyography system (SX230, Biometrics, Newport, UK). The spring force was measured by a single-axis load cell (FL25, Forsentek). The ground reaction force was measured by the force plate (AMTI, Watertown, MA, USA).

We used the measured lower limb segments motion and reaction force measured by the force plate to calculate the lower limb joint torque and joint power through inverse dynamics algorithm [40] (PlugInGait, Vicon). The biological torque and power of hip and knee joints were obtained by subtracting exoskeleton torque/power on the hip and knee joint from the total hip and knee joint torque/power. Muscle activities of each trial were rectified and low-pass filtered (fourth-order Butterworth, cut-off frequency 6 Hz) in the software (MATLAB 2018b, Mathworks). The metabolic rate was calculated from the average carbon dioxide and oxygen rate in the last 2 minutes using a Brockway equation [41]. The net metabolic rate was obtained by subtracting the metabolic rate of quiet standing from total metabolic rate of walking.

The spring force, joint angle, joint torque, joint power and muscle activity of each trial were divided into gait cycles, defined as the subsequent heel strikes of the same leg. We first obtained an average curve for each person and condition. For each participant, average muscle activity and average exoskeleton torque were calculated as the time integral of muscle activity and exoskeleton torque divided by time of gait cycle for each condition. Average muscle activity and exoskeleton torque during the assistive period were calculated as the time integral of muscle activity and exoskeleton torque

during assistive period divided by the time of the gait cycle. We normalized muscle activity of each muscle by dividing maximum value during NE condition. After obtaining the average spring force, muscle activity, and joint angle for each person, the data were averaged across participants for each condition.

G. Statistics

As the net metabolic rate, average muscle activity and peak extension/flexion angle data followed the normal distribution according to Jarque-Bera test (all $p > 0.05$; Matlab 2018b), mixed-model, two-way ANOVA (random effect: participant; fixed effects: spring stiffness) was conducted on net metabolic reduction, average muscle activity and peak extension/flexion angle data across conditions to verify the effect of spring stiffness (significance level $\alpha = 0.05$; Matlab 2018b, Mathworks). For each condition, means and standard errors of net metabolic rate, average muscle activity and peak extension/flexion angle were calculated across participants. After the ANOVA test, we used a two-sided paired t-test with Holm-Šidák correction to compare spring conditions to no exoskeleton (NE) condition to find which spring condition showed a significant change. A least-squares regression was used to fit a second-order polynomial (quadratic) function relating mean metabolic rate to spring stiffness. We also performed F-test on the regression model to determine whether the mean metabolic rate and spring stiffness had a significant quadratic relationship.

III. Results

As shown in Fig. 3, the energy storage phase of the exoskeleton (phase I) started at nearly 89% gait cycle (GC) and covered the biceps femoris muscle activation interval. With the regulation of bi-articular energy by the exoskeleton, the target biceps femoris and gluteus maximus average activity (bi-articular muscle, major hip extensor and knee flexors) decreased ($p = 0.011$, $p = 0.036$) during the whole gait cycle (Fig. 3e-f). During Phase I, the exoskeleton spring spanning hip and knee joints recycles energy from the knee joint, passively providing knee and hip with flexion and extension torque respectively. The target biceps femoris activity (bi-articular muscle, major hip extensor and knee flexors) mainly decreased ($p < 0.001$) in this phase. The gluteus maximus activity (mono-articular muscle, major hip extensor) mainly decreased when the stored energy was released to assist hip extension. The exoskeleton torque on hip and knee joint increased with the increasing spring stiffness ($p < 0.01$). The average positive exoskeleton power on hip joint ($p < 0.01$) and average negative exoskeleton power on knee joint ($p < 0.01$) increased with the increasing spring stiffness. Unexpectedly, the exoskeleton performs negative mechanical work on hip joint before the energy storage phase due to pretension of spring and tension of ratchet torsion spring. The exoskeleton also performs a little amount of negative mechanical work on hip joint during energy releasing phase. The negative mechanical work of exoskeleton may partly offset the assistance effect.

As shown in Fig. 4, the biological joint torque and joint power were reduced with the assistance, which showed the same trend as the reduced target muscle activities in treadmill experiment. Both average negative power of knee joint and average positive power were reduced ($p < 0.001$, $p = 0.043$) during the assistive period. The reduction of target muscle activities and joint mechanics indicated that the bi-articular metabolic energy was regulated by the exoskeleton toward a more energy-effective direction, which was the direct reason for overall metabolic reduction during walking. The exoskeleton only performs positive work on the hip joint during assistive period, but the exoskeleton also performs negative mechanical work on hip joint before the energy storage phase due to pretension of spring and tension of ratchet torsion spring. Future work may include reducing the negative mechanical work on hip joint by selecting springs with smaller pretension.

The metabolic rate was reduced with the assistance of the exoskeleton with proper spring stiffness. As shown in Fig. 5a, the net metabolic rates showed a U shape in exoskeleton conditions within the tested range of spring stiffness. The relationship between the spring stiffness and net metabolic rate can be best fit to a quadratic model (N = 9; $y = 0.0658x^2 - 0.3401x + 3.8949$; y (W/kg), x (N·m Rad^{-1}); $R^2 = 0.95$; ANOVA with quadratic model, $p = 0.046$). The optimal spring stiffness of the exoskeleton was 270 N·m Rad^{-1}, corresponding to 8.6 ± 1.5% (mean ± s.e.m; paired t-test, $p < 0.001$) metabolic reduction compared to walking without exoskeleton. The net metabolic rate of NA did not show a significant increase compared to NE condition ($p = 0.1$), which indicated that exoskeleton mass did not cause significant metabolic penalty. In the speed experiment, as shown in Fig. 5b, the results showed that the net metabolic rate can be reduced with the assistance compared to walking with no exoskeleton at speed of 1.25 m s^{-1}, 1.5 m s^{-1} and 1.75 m s^{-1} ($p = 0.001$; $p < 0.001$; $p < 0.001$), which indicated that the proposed assistive principle could be applied at different walking speeds.

Although the exoskeleton only assisted hip and knee joints, the mechanics of lower limb joints were also altered as a whole. As shown in Fig. 3g, the gastrocnemius (bi-articular muscle, major ankle plantar-flexor and knee flexor) activity increased in the late stance phase ($p = 0.0208$). However, soleus activity, which is also the major ankle plantar-flexor, did not show a significant difference under the assistance ($p > 0.05$). In the force plate experiment, the ankle joint torque and power of optimal stiffness was increased compared to NE condition, which is the same trend as gastrocnemius activity changes. The activity of anterior tibialis (major ankle dorsiflexor) and rectus femoris (major hip flexor) remained unchanged ($p > 0.5$, $p > 0.5$).

As shown in Fig. 6, except the peak knee extension angle remained unchanged ($p = 0.08$), the other peak joint angles showed a significant difference across walking conditions in the treadmill experiment. For the optimal stiffness of 270 N·m Rad^{-1}, the peak hip flexion angle decreased (paired t-test, $p < 0.01$), peak hip extension angle increased (paired t-test, $p = 0.016$), peak ankle plantarflexion angle increased (paired t-test, $p = 0.027$) compared to NE condition. In the force plate experiment, the preferred walking speed of 270 N·m Rad^{-1}

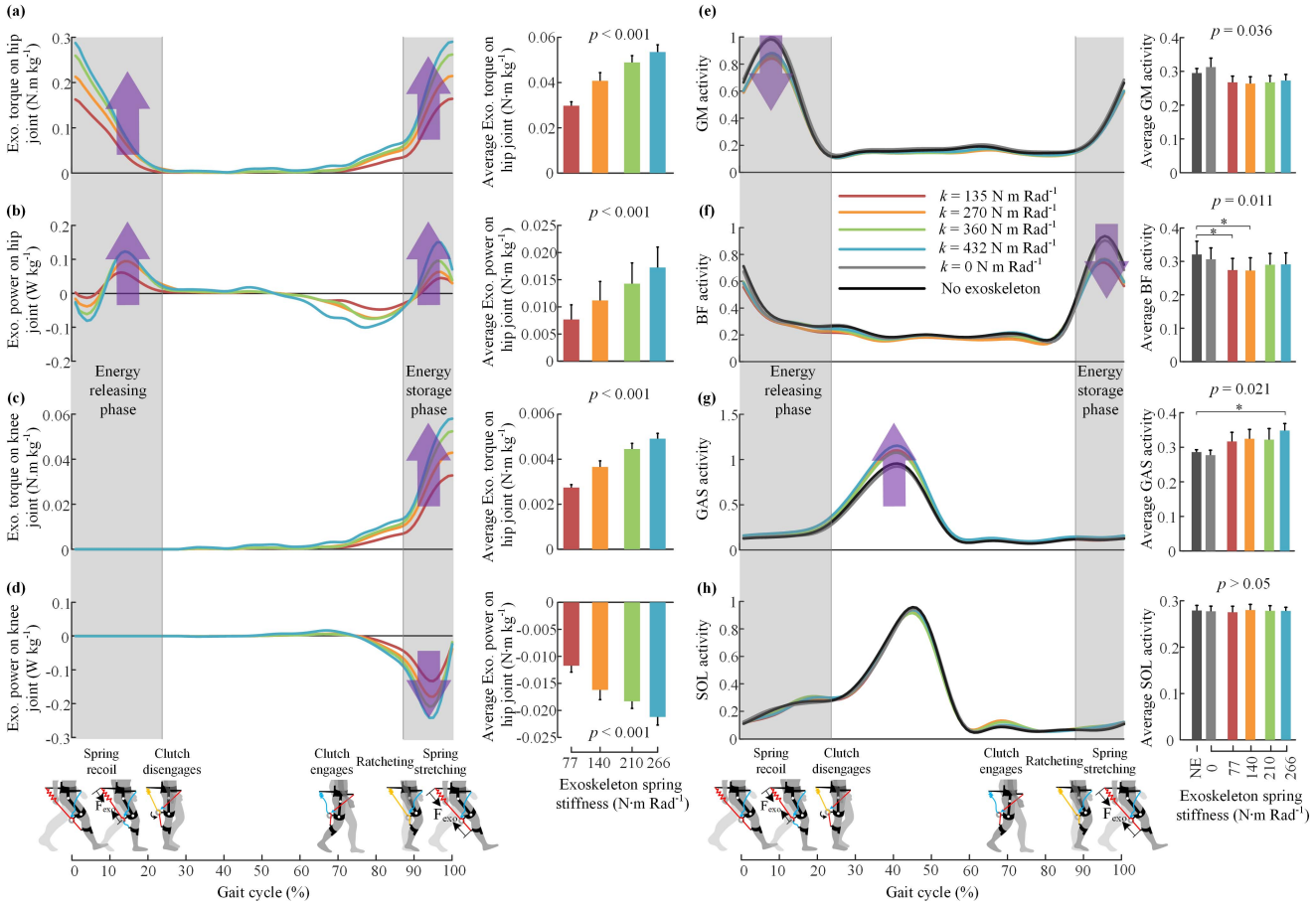

Fig. 3. **Exoskeleton torque and muscle activity in the treadmill experiment.** (a)-(d) Exoskeleton torque and power (normalized to body weight) on hip joint and knee in a gait cycle for each spring stiffness condition, averaged across participants. Shaded intervals represent approximate assistive intervals. Bar graphs on the right are the averages of the exoskeleton torque and power in the assistive interval. With the increasing spring stiffness, the exoskeleton torque and spring preload increased. Exoskeleton spring torque was generated at 70% GC due to the pretension force of spring stretched by slow extension of knee joint. We set the inflection point of the rising torque curve as the start timing of energy storage phase. (e)-(h) Muscle activities in gluteus maximus (GM), biceps femoris (BF), gastrocnemius (GAS), soleus (SOL). Bar graphs on the right are the averages of the muscle activities in the whole gait cycle. The biceps femoris (bi-articular muscle) and gluteus maximus (mono-articular) activity decreased in the assistive conditions compared to NE condition, mainly in assistive interval. The gastrocnemius (major ankle plantar-flexor, bi-articular muscle) activity increased in assistive conditions compared to NE condition, mainly during push-off. The soleus (mono-articular muscle) which is also major ankle plantar-flexor showed no significant change. $N = 9$; error bars, s.e.m; p values are the results of ANOVA tests on spring stiffness effect. NE, walking with no exoskeleton. Asterisks indicate significant differences relative to the NE condition (two-sided paired t-test with Holm-Šidák correction).

was 1.09 ± 0.02 m s^{-1}, similar to 1.10 ± 0.03 m s^{-1} of walking without exoskeleton ($p > 0.5$).

IV. Discussions

Previous studies have demonstrated that the metabolic rates of walking and running can be reduced with the assistance of mono-articular unpowered exoskeletons [15], [42] compared to walking/running without exoskeleton. In this paper, the proposed exoskeleton regulated hip and knee energy by recycling negative mechanical energy and transferring it to assist hip extension. The proposed exoskeleton regulated energy in a complementary manner that may not be exhibited by bi-articular muscles. By regulating hip and knee energy effectively, the overall metabolic energy of walking was reduced by 8.6 ± 1.5% compared to walking without exoskeleton.

In the previous study on unpowered multiarticular exoskeleton, the researchers found that the natural biomechanics of ankle joint was significantly altered with the coupled assistance of exoskeleton [13], possibly due to the fact that exoskeleton only focused on the function of energy recycling for multiple joints. In the recent study, people attach more importance on the energy transfer assistance of multiarticular prostheses [43], multiarticular powered exoskeleton [10] and (quasi-)passive exoskeletons [8], [21], [44]. It has been shown that the joint torque of the biological ankle joint can be reduced by transferring the energy from the knee joint to the ankle joint [21]. The experimental results also indicated that the metabolic cost can be reduced compared to wearing the exoskeleton with no assistance condition [44]. However, even the most advanced multiarticular unpowered exoskeletons that provide assistance have not been demonstrated to reduce metabolic cost compared with no exoskeleton due to the metabolic penalty of the exoskeleton mass and misalignment between exoskeleton structure and biological joint [17], [44]. We placed most of the exoskeleton mass near the trunk and adopt the design of separate thigh and shank parts to reduce

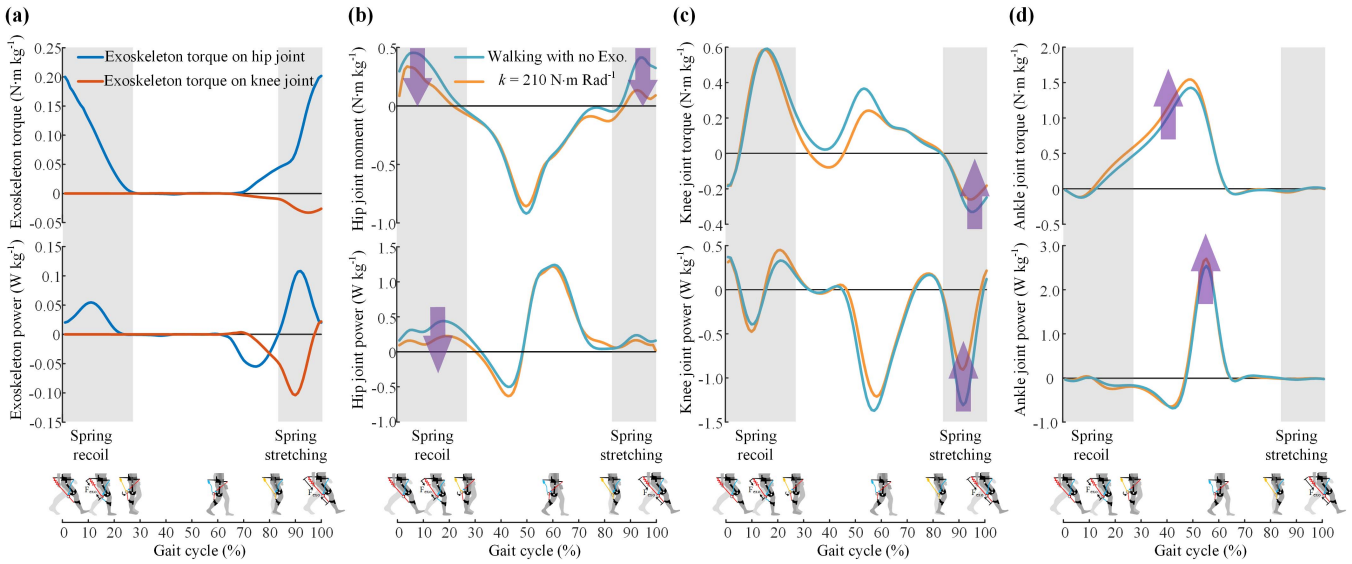

Fig. 4. **Exoskeleton mechanics and biological joint mechanics in the force plate experiment.** (a) Exoskeleton torque and power on hip joint and knee joint. (b)-(d) Biological joint moment and power in walking with no exoskeleton condition and 210 N·m Rad^{-1} condition. Biological moment/power in 210 N·m Rad^{-1} condition is equal to the measured moment/power minus the exoskeleton torque/power. Changes in joint mechanics showed the same trend to the changes in muscle activities in the treadmill experiment. During assistive periods (shaded periods), average hip positive power decreased (two-sided paired t-test, $p = 0.043$) compared to walking with no exoskeleton. During energy storage phase, average negative power of knee joint decreased ($p < 0.001$) compared to walking with no exoskeleton. The peak ankle plantarflexion power increased ($p = 0.004$) compared to walking with no exoskeleton, which is consistent with the trend of increased gastrocnemius muscle activity in the treadmill experiment.

the metabolic penalty and overcome misalignment problems. Besides, the proposed mechanical clutch is directly controlled by the hip joint angle. When the hip joint is extended to the hip extension posture, the pawl control string becomes taut, and only needs a small force to pull the pawl to directly control the clutch's disengagement. This direct control method of clutch engagement and disengagement was demonstrated to be reliable. As a result, our clutch did not fail during the experiment. The experimental results verify that lightweight mechanical structure and reliable control method together ensure the effectiveness of the proposed assistive principle.

The metabolic rate showed a U-shaped change with the increasing spring stiffness, which was similar to the results of a previous parameter sweep study on an unpowered ankle exoskeleton [15] and tethered active exoskeleton [8]. However, the reasons for metabolic reduction and return to normal levels are not identical. In the study of an ankle unpowered exoskeleton, the target soleus activity decreased during the energy storage phase of the exoskeleton. The soleus isometrically contracts while stretching the Achilles tendon during this phase [45]. Therefore, the authors inferred that the decreased target soleus activity resulted in a decreased muscle force, which was the major reason for metabolic reduction [15]. For our exoskeleton, the target biceps femoris and gluteus maximus activities decreased during energy storage and energy release phases, respectively. Compared to the soleus, the biceps femoris and gluteus maximus do not work with long elastic biological tendons, leading to low fixed-end compliance. The biceps femoris and gluteus maximus tend to contract eccentrically or concentrically to perform mechanical work with substantial metabolic cost [29]. Therefore, the muscle activity reduction was more likely to lead to a reduction in muscle work in both energy storage phase and energy release phases. The hip and knee joint power in force plate experiment showed a decreasing trend similar to that of the target muscle activities in treadmill experiment, supporting that the reduction in muscle work might result in the metabolic reduction.

With stiff spring assistance, the metabolic rate returned to a normal level. In our experiment, the muscle (rectus femoris) activity counteracting the assistive torque did not significantly increase during the energy storage phase of the exoskeleton as observed in a previous study on ankle unpowered exoskeleton [15]. A possible insight into the metabolic return to normal level might be that gastrocnemius muscle activity increased in the late stance phase and early swing phase (Fig. 3g). During walking, both hip and ankle joints play important roles in supporting the body mass, propelling the body center of mass (COM) and changing the kinetic energy of the limb. The ankle push-off actuated by ankle plantar flexors not only contributes to COM acceleration but also contributes to leg swing [46], which is performed synergistically with the flexors [47]. As the exoskeleton spring absorbed part of the mechanical energy in the swing phase, the muscle activity results showed that the participants tended to increase the muscle activity of the ankle plantar-flexors but not hip flexors activity to provide additional energy input for exoskeleton. In the stiff spring condition, excessive energy storage in the spring led to an unexpected increase in gastrocnemius activity to generate additional energy, thus offsetting the effect of the assistance. Although both the soleus and gastrocnemius are major plantar-flexors, the soleus muscle activity did not change significantly during push-off. This finding was possibly due to the different energetic function between soleus and gastrocnemius. A previous study indicated that the energy produced by

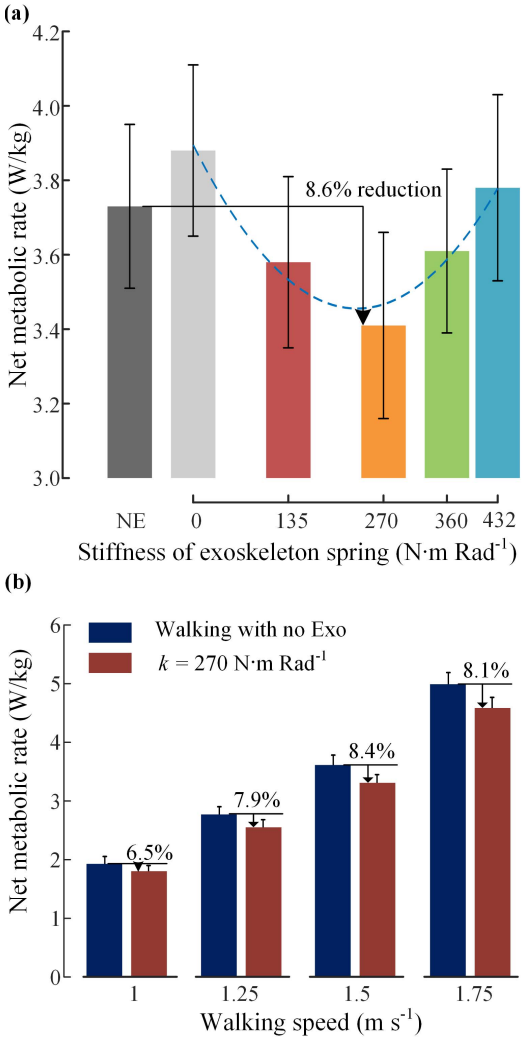

Fig. 5. **Changes in net metabolic rate.** (a) The net metabolic rate of exoskeleton conditions was significantly affected by spring stiffness (N = 9; mixed-model ANOVA, $p < 0.001$). The net metabolic rate was first decreased then increased with the increasing spring stiffness compared to walking with no exoskeleton condition (NE). The dashed line is the quadratic best fit to mean net metabolic rate from spring stiffness ($R^2 = 0.95$; $p = 0.046$). Changes in net metabolic rate was 0.32 ± 0.06 W kg^{-1} (mean $\pm$ s.e.m) under 270 N·m Rad^{-1} condition, which was equal to $8.6 \pm 1.5\%$ reduction compared to NE condition (two-sided paired t-test; $p < 0.001$). The net metabolic rate of walking with exoskeleton but no assistance (NA) and 432 N·m Rad^{-1} condition remained unchanged compared to NE condition (paired t-test; $p = 0.1$, $p = 0.6$). (b) The net metabolic rates were reduced with the assistance of exoskeleton compared to walking with no exoskeleton at speeds of 1.25 m s^{-1} ($N = 9$; two-sided paired t-test, $p = 0.001$), 1.5 m s^{-1} ($p < 0.001$), 1.75 m s^{-1} ($p < 0.001$). The metabolic rate showed a trend of reduction compared to walking with no exoskeleton ($p = 0.08$).

the soleus is delivered to accelerate trunk forward and that the energy of gastrocnemius was almost used for leg swing initiation [48]. We also found that the metabolic rate showed an increase trend in k = 0 N m rad^{-1} condition compared to NE condition, possibly due to the metabolic penalty caused by exoskeleton mass. We may reduce the metabolic penalty of exoskeleton mass by using lighter materials, such as carbon fiber [15]. On the other hand, since the clutch was attached to the thigh brace, metabolic energy penalties of the clutch is 3.87 W (mass∗metabolic penalty coefficients, metabolic penalty coefficients are summarized in [7]), which was even higher than that of the waist frame (2.76 W). Therefore, we may reduce the metabolic penalty by designing a more compact and lightweight mechanical clutch.

The joint angles of the participants significantly changed with the assistance of exoskeleton compared to walking without exoskeleton. This finding was also observed in previous studies [10], [49]. The kinematic changes might be the results of the participants adapting to the exoskeleton assistance and may also contribute the metabolic reduction, supporting that preserving the kinematics observed without assistance is not necessarily optimal for reducing the metabolic cost [49]. The force plate experiment simulated the situation of human walking freely on the level road. With the assistance of exoskeleton, the preferred walking speed did not significantly change, which indicates that the preferred walking speed did not decrease significantly when the exoskeleton exerted an opposing force on the knee joint during the leg swing.

Although the experimental results indicate that the metabolic cost of walking is reduced compared to normal walking, we acknowledge that there are still some limitations to this study. First, we inferred from low fixed end compliance characteristics of hip muscle-tendons and reduced muscle activity that the exoskeleton reduced the muscle work, thus reducing the metabolic cost. However, the exact changes in the underlying muscle dynamics remain unknown. Further insight may be gained by conducting additional experiments using in vivo ultrasound imaging techniques [50], [51]. Second, when the hip joint was in the hip extension posture, the hip string pulled the ratchet pawl and disengaged the mechanical clutch. We used a reset torsion spring in the pawl. When the hip extends to maximum extension position, the peak force in the hip string was 4 N, measured using a load cell. The hip flexion torque produced by the torsion spring in the ratchet pawl was very small and can be ignored. However, it may be a good idea to increase the torsion spring stiffness or use elastic elements in place of the pawl control string. As shown in Fig. 4, when the hip extends from upright position to maximum extension position, the biological hip joint torque is a flexion torque. Previous studies have indicated that the metabolic cost can be reduced with assistance of passive spring that is stretched during hip extension and released in hip flexion [31], [32]. We will explore this possibility in future work. Finally, although our exoskeleton provides assistance for only the knee and hip joints, the biological torque of ankle joint showed an increasing trend during push-off, which may be caused by the transfer of energy from the ankle musculature to the knee musculature. If we want to reduce the metabolic cost using the proposed exoskeleton further, additional assistance may be needed for ankle joint to reduce the biological torque and power during push-off. Previous studies on both unpowered ankle exoskeleton [15] and ankle powered exoskeleton [4] showed that the biological ankle power can be reduced with the assistance. Therefore, future work may include combining the proposed hip-knee passive exoskeleton with an ankle powered exoskeleton or ankle unpowered exoskeleton to further reduce the metabolic cost of walking.

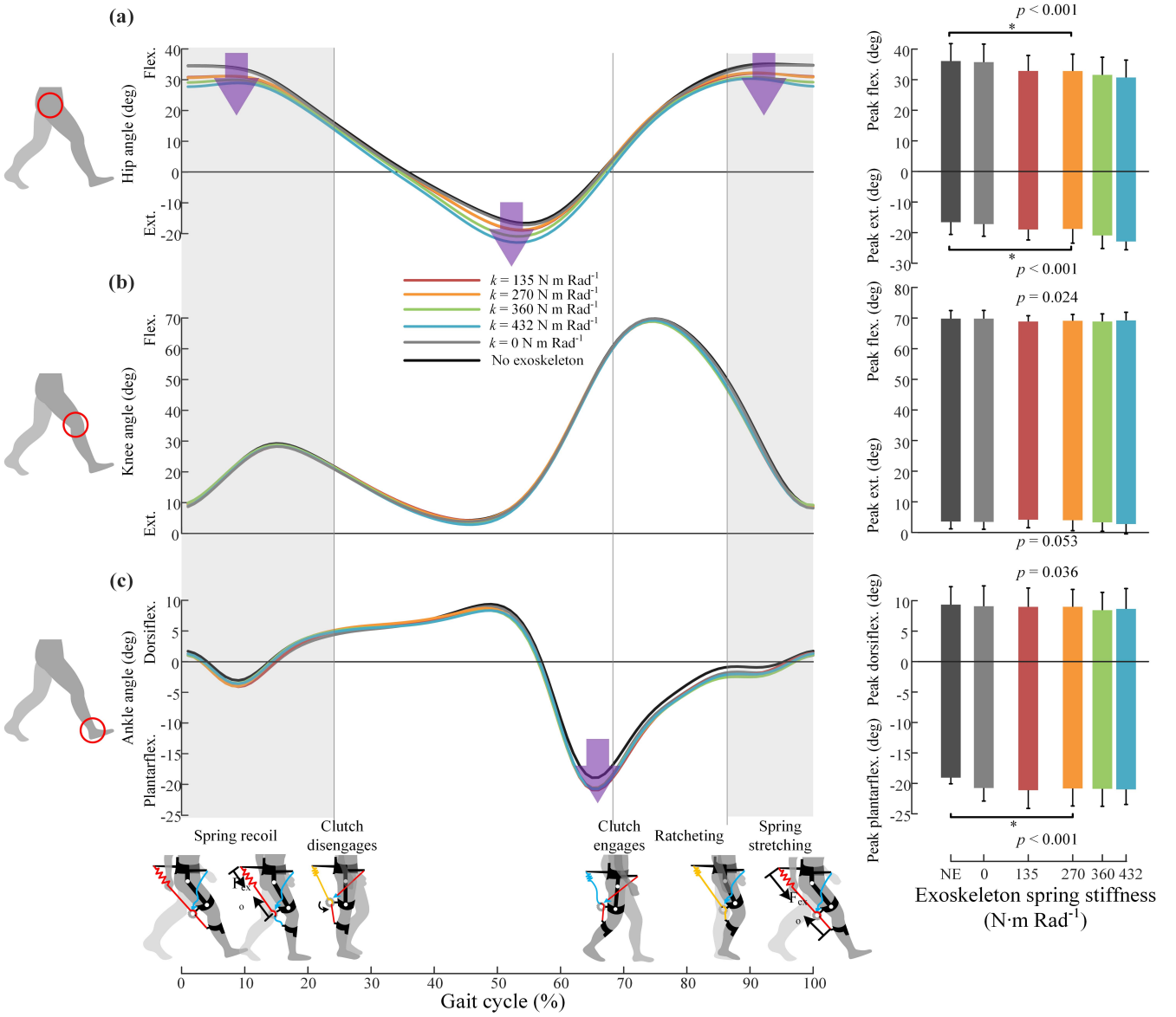

Fig. 6. **Joint kinematics in the treadmill experiment.** (a)-(c) The joint angles of hip, knee and knee in sagittal plane in a gait cycle. The trajectories are averaged across 9 participants for assistive conditions, NE and NA conditions. The bars at right are the peak values of these curves in a gait cycle. N = 9; error bars, s.e.m; p values are the results of ANOVA tests for effect on exoskeleton spring stiffness. Maximum hip flexion and extension decreased and increased respectively with the increasing spring stiffness (mixed model ANOVA, $p < 0.001$, $p < 0.001$). Maximum knee flexion, ankle dorsiflexion and ankle plantarflexion showed significant difference across conditions ($p = 0.024$, $p = 0.036$, $p < 0.01$). Asterisks (*) indicate significant differences between 270 N·m Rad^{-1} condition compared with NE condition.

V. Conclusion

We found that the metabolic rate was reduced by 8.6% with the assistance of a hip-knee unpowered exoskeleton that recycled and transferred energy in a complementary manner. The multiarticular unpowered exoskeleton was demonstrated to enhance multiarticular energy efficiency and reduce the metabolic cost compared to walking without exoskeleton. With effective energy transfer between lower limb joints, we have broken through the limitation of improving single-joint energy efficiency and found a way to regulate multiarticular metabolic energy to improve overall walking economy. The proposed design method that phased optimizes multiarticular energy efficiency may inspire future exoskeleton designs. The experimental results also provide a new insight into human responses to multiarticular passive assistance. Although the targeted joints were hip and knee joints, the mechanics of ankle musculature was altered to adapt assistance. A clear understanding of the human responses as a whole is essential for improving exoskeletons.

References

[1] H. Pontzer, "Economy and endurance in human evolution," *Current Biol.*, vol. 27, no. 12, pp. R613–R621, Jun. 2017.
[2] G. S. Sawicki, C. L. Lewis, and D. P. Ferris, "It pays to have a spring in your step," *Exerc. Sport Sci. Rev.*, vol. 37, no. 3, pp. 130–138, Jul. 2009.
[3] G. S. Sawicki, O. N. Beck, I. Kang, and A. J. Young, "The exoskeleton expansion: Improving walking and running economy," *J. Neuroeng. Rehabil.*, vol. 17, no. 1, p. 9, Feb. 2020.

[4] L. M. Mooney, E. J. Rouse, and H. M. Herr, "Autonomous exoskeleton reduces metabolic cost of human walking during load carriage," *J. Neuroeng. Rehabil.*, vol. 11, no. 1, p. 80, May 2014.

[5] K. Seo, J. Lee, Y. Lee, T. Ha, and Y. Shim, "Fully autonomous hip exoskeleton saves metabolic cost of walking," in *Proc. IEEE Int. Conf. Robot. Autom. (ICRA)*, May 2016, pp. 4628–4635.

[6] S. Lee *et al.*, "Autonomous multi-joint soft exosuit with augmentation-power-based control parameter tuning reduces energy cost of loaded walking," *J. Neuroeng. Rehabil.*, vol. 15, no. 1, pp. 1–9, Jul. 2018.

[7] J. Kim *et al.*, "Reducing the metabolic rate of walking and running with a versatile, portable exosuit," *Science*, vol. 365, no. 6454, pp. 668–672, Aug. 2019.

[8] P. Malcolm, W. Derave, S. Galle, and D. De Clercq, "A simple exoskeleton that assists plantarflexion can reduce the metabolic cost of human walking," *PLoS ONE*, vol. 8, no. 2, Feb. 2013, Art. no. e56137.

[9] A. J. Young, J. Foss, H. Gannon, and D. P. Ferris, "Influence of power delivery timing on the energetics and biomechanics of humans wearing a hip exoskeleton," *Frontiers Bioeng. Biotechnol.*, vol. 5, p. 4, Mar. 2017.

[10] B. T. Quinlivan *et al.*, "Assistance magnitude versus metabolic cost reductions for a tethered multiarticular soft exosuit," *Sci. Robot.*, vol. 2, no. 2, Jan. 2017, Art. no. eaah4416.

[11] J. Zhang *et al.*, "Human-in-the-loop optimization of exoskeleton assistance during walking," *Science*, vol. 356, no. 6344, pp. 1280–1283, Jun. 2017.

[12] Y. Ding, M. Kim, S. Kuindersma, and C. J. Walsh, "Human-in-the-loop optimization of hip assistance with a soft exosuit during walking," *Sci. Robot.*, vol. 3, no. 15, Feb. 2018, Art. no. eaar5438.

[13] W. van Dijk and H. Van der Kooij, "XPED2: A passive exoskeleton with artificial tendons," *IEEE Robot. Autom. Mag.*, vol. 21, no. 4, pp. 56–61, Dec. 2014.

[14] T. G. Sugar, K. W. Hollander, and J. K. Hitt, "Walking with springs," *Proc. SPIE*, vol. 7976, Mar. 2011, Art. no. 797602.

[15] S. H. Collins, M. B. Wiggin, and G. S. Sawicki, "Reducing the energy cost of human walking using an unpowered exoskeleton," *Nature*, vol. 522, no. 7555, pp. 212–215, Jun. 2015.

[16] C. J. Walsh, K. Endo, and H. Herr, "A quasi-passive leg exoskeleton for load-carrying augmentation," *Int. J. Humanoid Robot.*, vol. 4, no. 3, pp. 487–506, Sep. 2007.

[17] H. Barazesh and M. A. Sharbafi, "A biarticular passive exosuit to support balance control can reduce metabolic cost of walking," *Bioinspiration Biomimetics*, vol. 15, no. 3, Mar. 2020, Art. no. 036009.

[18] R. C. Browning, J. R. Modica, R. Kram, and A. Goswami, "The effects of adding mass to the legs on the energetics and biomechanics of walking," *Med. Sci. Sports Exerc.*, vol. 39, no. 3, pp. 515–525, Mar. 2007.

[19] K. Junius, M. Moltedo, P. Cherelle, C. Rodriguez-Guerrero, B. Vanderborght, and D. Lefeber, "Biarticular elements as a contributor to energy efficiency: Biomechanical review and application in bio-inspired robotics," *Bioinspiration Biomimetics*, vol. 12, no. 6, Nov. 2017, Art. no. 061001.

[20] P. Malcolm, S. Galle, W. Derave, and D. De Clercq, "Bi-articular knee-ankle-foot exoskeleton produces higher metabolic cost reduction than weight-matched mono-articular exoskeleton," *Frontiers Neurosci.*, vol. 12, p. 69, Mar. 2018.

[21] Y. Chang, W. Wang, and C. Fu, "A lower limb exoskeleton recycling energy from knee and ankle joints to assist push-off," *J. Mech. Robot.*, vol. 12, no. 5, pp. 1–17, Oct. 2020.

[22] A. V. Voronov, "The roles of monoarticular and biarticular muscles of the lower limbs in terrestrial locomotion," *Human Physiol.*, vol. 30, no. 4, pp. 476–484, Jul. 2004.

[23] L. Gregoire, D. Veeger, P. Huijing, and G. Schenau, "Role of mono- and biarticular muscles in explosive movements," *Int. J. Sports Med.*, vol. 5, pp. 301–305, Jan. 1985.

[24] B. I. Prilutsky and V. M. Zatsiorsky, "Tendon action of two-joint muscles: Transfer of mechanical energy between joints during jumping, landing, and running," *J. Biomech.*, vol. 27, no. 1, pp. 25–34, Jan. 1994.

[25] G. J. van Ingen Schenau, M. F. Bobbert, and A. J. van Soest, "The unique action of bi-articular muscles in leg extensions," in *Multiple Muscle Systems*. New York, NY, USA: Springer, 1990.

[26] B. I. Prilutsky, L. N. Petrova, and L. M. Raitsin, "Comparison of mechanical energy expenditure of joint moments and muscle forces during human locomotion," *J. Biomech.*, vol. 29, no. 4, pp. 405–415, Apr. 1996.

[27] R. P. Wells, "Mechanical energy costs of human movement: An approach to evaluating the transfer possibilities of two-joint muscles," *J. Biomech.*, vol. 21, no. 11, pp. 955–964, Jan. 1988.

[28] T. J. Roberts, "The integrated function of muscles and tendons during locomotion," *Comparative Biochem. Physiol. A, Mol. Integrative Physiol.*, vol. 133, no. 4, pp. 1087–1099, Dec. 2002.

[29] A. A. Biewener and T. J. Roberts, "Muscle and tendon contributions to force, work, and elastic energy savings: A comparative perspective," *Exerc. Sport Sci. Rev.*, vol. 28, no. 3, pp. 99–107, Jul. 2000.

[30] R. Margaria, "Positive and negative work performances and their efficiencies in human locomotion," *Internationale Zeitschrift für Angewandte Physiologie Einschließlich Arbeitsphysiologie*, vol. 25, no. 4, pp. 339–351, Dec. 1968.

[31] W. B. Chen, S. Wu, T. C. Zhou, and C. H. Xiong, "On the biological mechanics and energetics of the hip joint muscle–tendon system assisted by passive hip exoskeleton," *Bioinspiration Biomimetics*, vol. 14, no. 1, Jan. 2019, Art. no. 016012.

[32] F. A. Panizzolo, C. Bolgiani, L. Di Liddo, E. Annese, and G. Marcolin, "Reducing the energy cost of walking in older adults using a passive hip flexion device," *J. Neuroeng. Rehabil.*, vol. 16, no. 1, pp. 1–9, Oct. 2019.

[33] F. L. Haufe, P. Wolf, R. Riener, and M. Grimmer, "Biomechanical effects of passive hip springs during walking," *J. Biomech.*, vol. 98, Jan. 2020, Art. no. 109432.

[34] J. M. Donelan, Q. Li, V. Naing, J. A. Hoffer, D. J. Weber, and A. D. Kuo, "Biomechanical energy harvesting: Generating electricity during walking with minimal user effort," *Science*, vol. 319, no. 5864, pp. 807–810, Feb. 2008.

[35] B. R. Umberger, "Stance and swing phase costs in human walking," *J. Roy. Soc. Interface*, vol. 7, no. 50, pp. 1329–1340, Sep. 2010.

[36] P. S. Walker, H. Kurosawa, J. S. Rovick, and R. A. Zimmerman, "External knee joint design based on normal motion," *J. Rehabil. Res. Develop.*, vol. 22, no. 1, pp. 9–22, Jan. 1985.

[37] C. Xiong, T. Zhou, L. Zhou, T. Wei, and W. Chen, "Multi-articular passive exoskeleton for reducing the metabolic cost during human walking," in *Proc. Wearable Robot. Assoc. Conf.*, Mar. 2019, pp. 63–67.

[38] K. Shamaei, G. S. Sawicki, and A. M. Dollar, "Estimation of quasi-stiffness of the human hip in the stance phase of walking," *PLoS ONE*, vol. 8, no. 12, Dec. 2013, Art. no. e81841.

[39] K. Shamaei, G. S. Sawicki, and A. M. Dollar, "Estimation of quasi-stiffness of the human knee in the stance phase of walking," *PLoS ONE*, vol. 8, no. 3, Mar. 2013, Art. no. e59993.

[40] D. Winter, *Biomechanics and Motor Control of Human Movement*, 4th ed. Hoboken, NJ, USA: Wiley, Sep. 2009.

[41] J. M. Brockway, "Derivation of formulae used to calculate energy expenditure in man," *Hum. Nutrition, Clin. Nutrition*, vol. 41, no. 6, pp. 71–463, Nov. 1987.

[42] R. Nasiri, A. Ahmadi, and M. N. Ahmadabadi, "Reducing the energy cost of human running using an unpowered exoskeleton," *IEEE Trans. Neural Syst. Rehabil. Eng.*, vol. 26, no. 10, pp. 2026–2032, Oct. 2018.

[43] L. Flynn, J. Geeroms, R. Limenez-Fabian, B. Vanderborght, N. Vitiello, and D. Lefeber, "Ankle–knee prosthesis with active ankle and energy transfer: Development of the CYBERLEGs alpha-prosthesis," *Robot. Auto. Syst.*, vol. 73, pp. 4–15, Nov. 2015.

[44] E. Etenzi, R. Borzuola, and A. M. Grabowski, "Passive-elastic knee-ankle exoskeleton reduces the metabolic cost of walking," *J. Neuroeng. Rehabil.*, vol. 17, no. 1, pp. 1–15, Jul. 2020.

[45] M. Ishikawa, P. V. Komi, M. J. Grey, V. Lepola, and G.-P. Bruggemann, "Muscle-tendon interaction and elastic energy usage in human walking," *J. Appl. Physiol.*, vol. 99, no. 2, pp. 603–608, Aug. 2005.

[46] K. E. Zelik and P. G. Adamczyk, "A unified perspective on ankle push-off in human walking," *J. Experim. Biol.*, vol. 219, no. 23, pp. 3676–3683, Dec. 2016.

[47] H. Sadeghi, S. Sadeghi, F. Prince, P. Allard, H. Labelle, and C. L. Vaughan, "Functional roles of ankle and hip sagittal muscle moments in able-bodied gait," *Clin. Biomech.*, vol. 16, no. 8, pp. 688–695, Oct. 2001.

[48] R. Neptune, S. Kautz, and F. E. Zajac, "Contributions of the individual ankle plantar flexors to support, forward progression and swing initiation during walking," *J. Biomech.*, vol. 34, no. 11, pp. 1387–1398, Nov. 2001.

[49] C. L. Lewis and D. P. Ferris, "Invariant hip moment pattern while walking with a robotic hip exoskeleton," *J. Biomech.*, vol. 44, no. 5, pp. 789–793, Mar. 2011.

[50] A. Lai, G. A. Lichtwark, A. G. Schache, Y.-C. Lin, N. A. T. Brown, and M. G. Pandy, "*In vivo* behavior of the human soleus muscle with increasing walking and running speeds," *J. Appl. Physiol.*, vol. 118, no. 10, pp. 1266–1275, May 2015.

[51] M. Ishikawa, J. Pakaslahti, and P. V. Komi, "Medial gastrocnemius muscle behavior during human running and walking," *Gait Posture*, vol. 25, no. 3, pp. 380–384, Mar. 2007.